Supporting Information for

Catalytic performance of Fe-based supported polyoxometalate catalyst in the oxidative cleavage of β-O-4 lignin model compounds

Danqi Wu,[a] Huihui Zhang,[b] Ji Ding,[a] Yanqin Wang,[a] Huiying Liao,[a] Dianyong Yang,[a] Pengfei An,[c] Li Guo,[d] Sheng Dai,[b] and Zhenshan Hou[a,]*

[a]State Key Laboratory of Green Chemical Engineering and Industrial Catalysis, Research Institute of Industrial Catalysis, School of Chemistry & Molecular Engineering., East China University of Science and Technology, Shanghai 200237, China. E-mail: houzhenshan@ecust.edu.cn, wangyanqin@ecust.edu.cn

[b]Key Laboratory for Advanced Materials and Feringa Nobel Prize Scientist Joint Research Center, Institute of Fine Chemicals, School of Chemistry & Molecular Engineering, East China University of Science and Technology, Shanghai 200237, China.

[c]Institute of High Energy Physics, Chinese Academy of Sciences, Beijing Synchrotron Radiation Facility (BSRF), Beijing 100049, China. E-mail: anpf@ihep.ac.cn

[d]Key Laboratory of Hubei Province for Coal Conversion and New Carbon Materials, School of Chemistry and Chemical Engineering, Wuhan University of Science and Technology, Heping Avenue 947, Wuhan 430081, China. E-mail: guoli@wust.edu.cn

1. Materials

All commercially available chemicals were used as received without further purification. Phosphomolybdic acid hydrate ($H_3PMo_{12}O_{40}\cdot nH_2O$) was obtained from Shanghai Naicheng Biotechnology Co., Ltd, hydrochloric acid (HCl), nickel nitrate hexahydrate ($NiNO_3\cdot 6H_2O$), cesium nitrate ($CsNO_3$), nitric acid (HNO_3), potassium nitrate (KNO_3) and acetone were obtained from China National Pharmaceutical Group Chemical Reagent Co., Ltd, ferric nitrate nonahydrate ($Fe(NO_3)_3\cdot 9H_2O$), ethanol, tetrahydrofuran (THF), sodium borohydride ($NaBH_4$), methanol and dimethyl sulfoxide (DMSO) were obtained from Shanghai Titan Technology Co., Ltd, copper nitrate trihydrate ($Cu(NO_3)_2\cdot 3H_2O$) was obtained from Beijing Yinuokai Technology Co., Ltd, cobalt nitrate hexahydrate ($Co(NO_3)_2\cdot 6H_2O$) was obtained from Shanghai Macklin Biochemical Co., Ltd, phenol was obtained from Meryer Technology Co., Ltd, 2-bromoacetophenone, 5,5-dimethyl-1-pyrrolin-n-oxide (DMPO) and 2,2,6,6-tetramethylpiperidine oxide (TEMPO) were obtained from Anhui Senrise Technology Co., Ltd, ethyl acetate was from Jiangsu Anhuai Chemical Technology Co., Ltd, ammonium chloride (NH_4Cl) was obtained from Shanghai Zhonghe Chemical Technology Co., Ltd, dimethyl sulfoxide-d$_6$ (DMSO-d$_6$) was obtained from Shanghai J&K Chemical Technology Co., Ltd, Oxygen (O_2) was obtained from Shanghai Shangnong Gas Co., Ltd, birch wood dust, acetonitrile and ammonium acetate were obtained from Shanghai D&B Biological Science and Technology Co., Ltd as mobile phases in high performance liquid chromatography (HPLC) analysis.

2. Experimental

2.1 Preparation of M (Fe, Co, Ni, Cu) / Cs-PMA

Taking 0.5% Fe/Cs-PMA as an example, phosphomolybdate hydrate (PMA) (2.0

g) was dissolved in ultra-pure water (40 ml) and acidified with 65-68% HNO_3 to get solution A. $CsNO_3$ (0.63 g) and Fe $(NO_3)_3 \cdot 9H_2O$ (13 mg) were dissolved in ultra-pure water (30 ml) and acidified with a few drops of concentrated HNO_3 to obtain solution B. Then, under the ice bath condition, solution B was added dropwise to solution A containing heteropoly acid with the drop rate of 1-2 ml$\cdot$ min^{-1}. During the drop process, yellow precipitates were gradually formed. The suspension was continuously stirred for 5 h under the ice bath condition. After that, the precipitated suspension was centrifuged, washing 3 times in ultra-pure water, dried, and carefully ground for use. Catalysts with different Fe content and other metals (Co, Cu) were prepared according to similar procedure. In order to obtain Fe-free POM, only cationic solution containing Cs^+ was co-precipitated with heteropoly acid solution containing POM.

2.2 Preparation of β-O-4 lignin model compounds and birch lignin

2.2.1 Synthesis of 2-phenoxy-1-phenylethanone (β-O-4 ketone)

Phenol and 2-bromoacetophenone were dissolved in acetone, then a certain amount of K_2CO_3 was added, and finally refluxed at 60 °C for 8h. After that, K_2CO_3 was removed by hot filtration and added $MgSO_4$ to the organic phase to remove H_2O, then the solvent was removed by evaporation and the solid was freeze-dried. Finally, the solid was dissolved in ethanol and recrystallized, and the β-O-4 ketone was obtained by vacuum drying at room temperature.

2.2.2 Synthesis of 2-phenoxy-1-phenylethanol (β-O-4 alcohol)

2-phenoxy-1-phenylethanol was synthesized by β-O-4 ketone liquid phase reduction manner. β-O-4 ketone was dissolved in methanol solution, and few amount of $NaBH_4$ was added and stirred at room temperature for 6 hours for reduction. After the reaction was completed, 1M saturated NH_4Cl solution was added for quenching. Next, ethyl acetate was added for extraction, washed with ultra-pure water, and then $MgSO_4$ was added to remove superfluous H_2O. Then the organic phase was removed by evaporation and 2-phenoxy-1-phenylethanol was obtained by vacuum extraction at room temperature. Other β-O-4 lignin model compounds were prepared in the similar method. All substrates were characterized by ^1H NMR hydrogen and ^{13}C NMR carbon spectra (Fig. S7-S11).

2.2.3 Preparation of birch lignin

Birch lignin was extracted by acid hydrolysis. Firstly, 60 mesh wood dust powder was dispersed in 3 wt% HCl methanol solution, followed by refluxing at 90°C for 3 days and fully stirred. After that, it was cooled to room temperature, filtering to remove the residual wood dust and remain the filtrate. Then, ice water was added, stirring it thoroughly for 5 hours to form reddish brown precipitate. Finally, the precipitate was filtered and washed, drying in the vacuum drying oven.

2.3 Catalytic Oxidative Cleavage of Lignin Model Compounds

The oxidation of β-O-4 model compounds was performed in a 50 mL high-pressure batch stainless-steel autoclave. Typically, 0.5 mmol of β-O-4 model compound, 50 mg catalyst was suspended in 3 mL DMSO and then the reactor was filled with O_2 3 times to exhaust the air. Finally, it was pressurized with O_2 to 1.0 MPa and heated to the specific temperature with sustaining stirring. After the reaction was completed, the autoclave was cooled to room temperature. O_2 was then slowly released and the reaction liquid was centrifuged. The supernatant was moved to the centrifuge tube and the used catalyst was dried to collect for the next cycle. The reaction solution was then analyzed by HPLC, using CH_3CN: H_2O= 7:3 and 0.02 M CH_3COONH_4: CH_3CN= 95:5 as the mobile phases.

$$\text{Conversion}=\frac{amount\ of\ substrates\ converted\ (mole)}{total\ amount\ of\ substrates\ (mole)}\times 100\%$$

(1)

$$\text{Yield}=\frac{\text{amount of products (mole)}}{\text{total amount of substrates (mole)}}\times 100\%$$

(2)

2.4 0.5% Fe/Cs-PMA-Catalyzed Decomposition of Birch Lignin

Decomposition of birch lignin was performed in a 50 mL high-pressure batch stainless-steel autoclave. Typically, 0.1 g birch lignin, 0.1 g 0.5% Fe/Cs-PMA was suspended in 5 mL DMSO and then the reactor was filled with 1MPa O_2, which would be heated to 140 ^{o}C with sustaining stirring. After the reaction completed, the autoclave was cooled to room temperature. O_2 was then slowly released and the catalyst was centrifuged. The products in upper solution were qualified by HPLC-MS and quantified specifically by HPLC with external standard curve, using CH_3CN: H_2O= 7:3 and 0.02 M CH_3COONH_4: CH_3CN= 95:5 as the mobile phases.

$$\text{Conversion}=\frac{Mass\ of\ lignin\ after\ reaction}{Mass\ of\ lignin\ before\ reaction}\times 100\%$$

(1)

$$\text{Yield}=\frac{\text{amount of products (mg)}}{\text{total amount of substrates (mg)}}\times 100\%$$

(2)

3. Catalyst characterization

Powder X-ray diffraction (XRD) patterns were performed in the 2θ range of 5-75° from Rigaku equipped with a 9-kW rotating anode Cu source at 45 kV and 100 mA. Fourier-transform FT-IR spectra were recorded from pressed KBr pellets at room temperature on a Nicolet Nexus 670 FT-IR spectrometer. Scanning transmission electron microscopy (STEM) characterization was performed on a ThermoFisher Talos F200X microscope under 200 kV. High angle annular dark field HAADF-STEM images were recorded using a convergence semi angle of 10.5 mrad, and inner- and outer collection angles of 59 and 200 mrad, respectively. Energy dispersive X-ray spectroscopy (EDS) was carried out using 4 in column Super-X detectors. X-ray photoelectron spectroscopy (XPS) was performed using Thermo Scientific K-Alpha. ^{1}H NMR were recorded on a Bruker Avance III 400 instrument (400 MHz for ^{1}H NMR) and ^{13}C NMR were recorded on Ascend 600 (151 MHz for ^{13}C NMR) using $CDCl_3$ as the solvent. The reaction products were analyzed by using High Performance Liquid Chromatography (HPLC) [a LC-100 Liquid Chromatograph with the GH0515046C18A column (150mm× 4.6mm), a UV detector at column temperature of 30 °C and flow rate of 0.5 mL/min (270 nm for phenol, PP-one, MB and MP detection) and 1.0 mL/min (230 nm for BA detection)].

Infrared (IR) spectra of pyridine adsorption were recorded on Nicolet NEXUS 670 FT–IR spectrometer. The samples were pressed into self-supporting disks and placed in an IR cell attached to a closed glass–circulation system. The disk was dehydrated by heating at 200 °C, for 1 h under vacuum in order to remove the physically adsorbed water. After the cell was cooled to room temperature, the IR spectrum was recorded as the background. Pyridine vapor was then introduced into the cell at room temperature until equilibrium was reached, and then a second spectrum was recorded. Subsequent evacuation was performed at 150 °C, 100 °C, 50 °C for 10 min respectively followed by spectral acquisitions. The spectra presented were obtained by subtracting the spectra recorded before and after pyridine adsorption.

H_2-TPR (30 mg sample loaded) and NH_3-TPD (60 mg sample loaded) were carried out on an Automatic temperature programmed adsorption instrument Finesorb-3010 with a thermal conductivity detector (TCD) in 10% H_2 /Ar and 10% NH_3/N_2 respectively.

X-ray absorption structure spectra (XAS), including X-ray absorption near-edge structure (XANES) and extended X-ray absorption fine structure (EXAFS) were collected at the beamline 1W1B of the Beijing Synchrotron Radiation Facility (BSRF), Institute of High Energy Physics (IHEP), Chinese Academy of Sciences (CAS). The Fe K-edge XANES data of Fe foil and Fe_2O_3 were recorded in transmission mode, while the data of 0.5% Fe/Cs-PMA and 0.5% Fe/Cs-PMA were recorded in fluorescence mode by Lytle. The storage ring worked at an energy of 2.5 GeV with an average electron current of below 200 mA. The acquired EXAFS data were extracted and processed according to the standard procedures using the FEFIT software packages implemented within the ATHENA module. The k^2-weighted Fourier transform (FT) of

$\chi(k)$ in R space was obtained over a range of 0-12.0 Å^{-1} by applying a Besse window function.

Two-dimensional HSQC spectra were acquired using a Bruker Advance 600-MHz from Huazhong University of Science and Technology. The experimental conditions were as follows: temperature 25°C; Pulse signal: 60°; Delay time: 2s; Scanning times: 30000 times.

For oxidative degradation of Birch lignin, the reaction solution was analyzed by HPLC-MS (Q Exactive Orbitrap LC-MS/MS system, Thermo Fisher Scientific), which equipped with the chromatographic column (Thermo Hypersil GOLD C18, 3μm, 2.1mm*100mm), secondary mass spectrometry mode (HCD) and electrospray ion source (ESI).

Table S1. Structural parameters of different catalysts extracted from the EXAFS fitting.

Sample	Path	CN.	R (Å)	σ^2 (10^{-3}A^2)	ΔE_0 (eV)	R factor (%)
Fe foil	Fe-Fe	8.0	2.47	1.27	10.33	1.8
Fe_2O_3	Fe-O	6.0	1.98	5.50	4.61	1.4
0.5% Fe/Cs-PMA	Fe-O	3.3±0.18	1.89	5.40	0.26	1.0
1.0% Fe/Cs-PMA	Fe-O	3.1±0.14	1.82	5.01	-0.44	1.6

C.N., R (Å), σ^2, ΔE_0 are the coordination number, interatomic distance, Debye-Waller factor, edge-energy shift. R factor is used to value the goodness of the fitting.

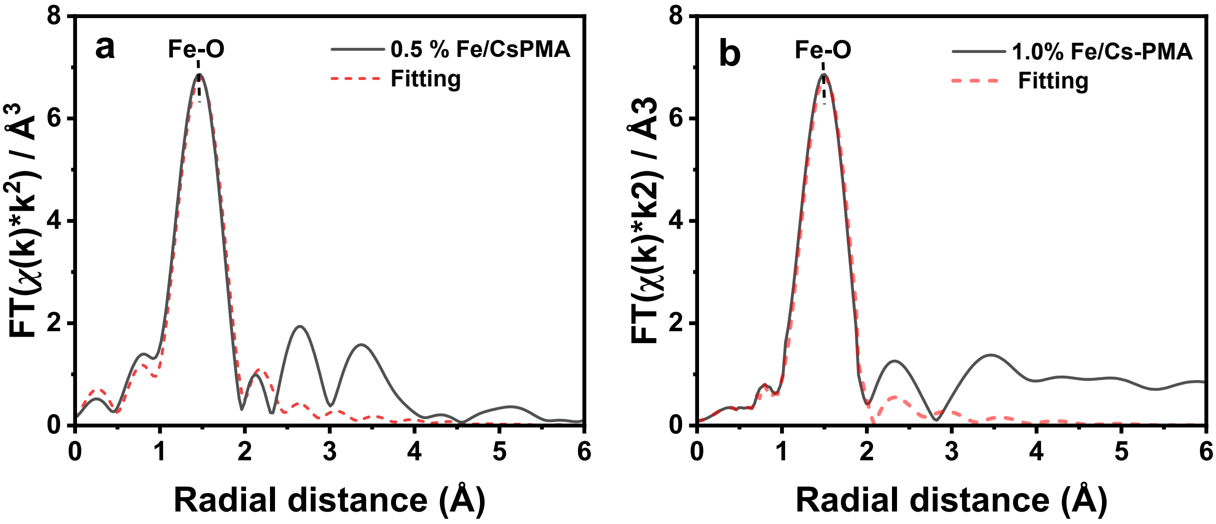

Fig S1. Fourier transforms of k_2-weighted Fe edge EXAFS experimental data for (a) 0.5 % Fe/Cs-PMA and (b) 1.0 % Fe/Cs-PMA and their EXAFS fitting curves at the R space.

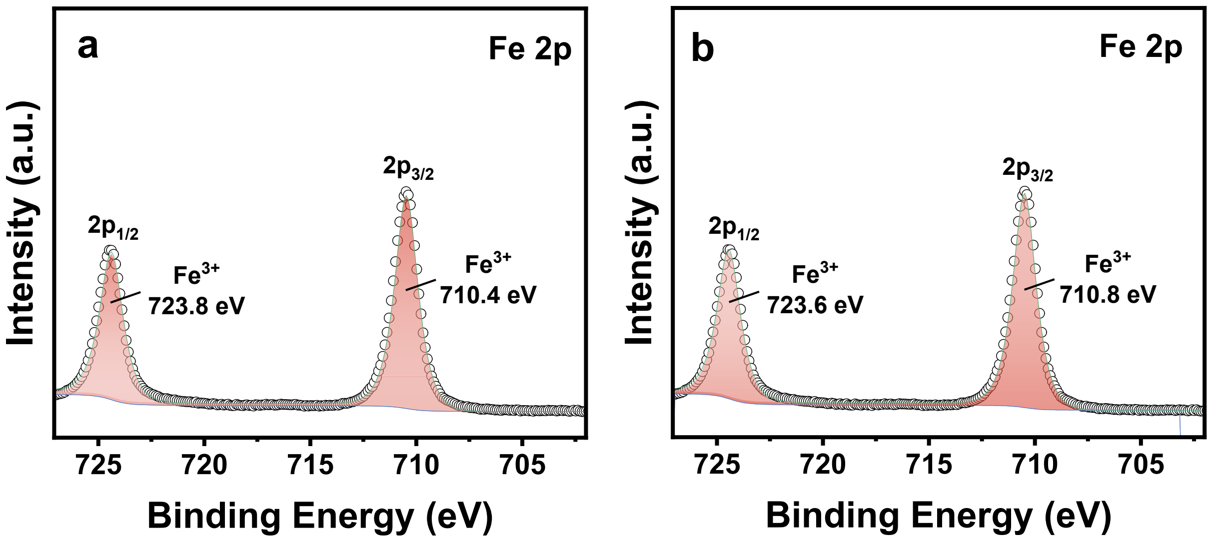

Fig S2. XPS spectra over 2.0% Fe/Cs-PMA of (a) before reaction and (b) after reaction.

Table S2. Physicochemical properties and FTIR of pyridine for oxidative cleavage of PP-ol.

Catalyst	M (g)	FTIR of pyridine		
		L (area/g)	B (area/g)	B/L
Cs-PMA	0.0942	2.5	52	20
0.5% Fe/Cs-PMA	0.0989	12	58	4.8
1.0% Fe/Cs-PMA	0.1073	25	64	2.6
2.0% Fe/Cs-PMA	0.0994	45	72	1.6
After reaction	0.0968	21	61	2.9

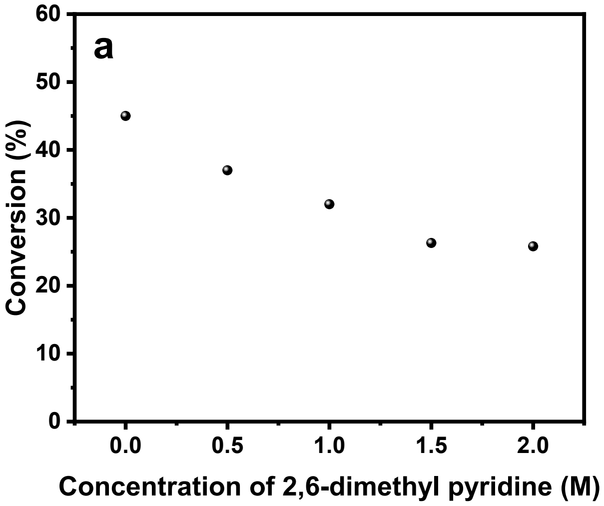

Fig. S3. Effect of (a) 2,6-dimethyl pyridine and (b) pyridine additive on the oxidation cleavage of PP-ol. Reaction conditions: 0.5 mmol PP-ol, 0.5 % Fe/Cs-PMA, 4 mL DMSO, 1 MPa O_2, 140 °C, 4 h.

Table S3. Comparison of the activity over various catalysts in oxidative reaction.

Catalyst	Substrate/main products	T /°C	Time /h	Conv. /%	Stability	Ref.
2.0% Pd/CeO_2	PP-ol/Phenol & BA& MB	185	24	64	5 cycles	1
1.0% RuMo/rGO	PP-ol/ Phenol & BA& MB	100	12	94	6 cycles	2
0.88% Au/CeO_2	PP-ol/ Phenol & BA& MB	180	4	71.5	4 cycles	3
$NLLH_5V_2Mo_{18}O_{62}$	PP-ol/ Phenol & BA	130	10	96	10 cycles	4
$HPMoV_2$	PP-ol/ Phenol & methoxylate	140	4	60	-	5
Bim-V-2	PP-ol/ Phenol & BA & MB	120	10	97	5 cycles	6
0.5% Fe/Cs-PMA	PP-ol/ Phenol & BA	140	12	99	5 cycles	This work

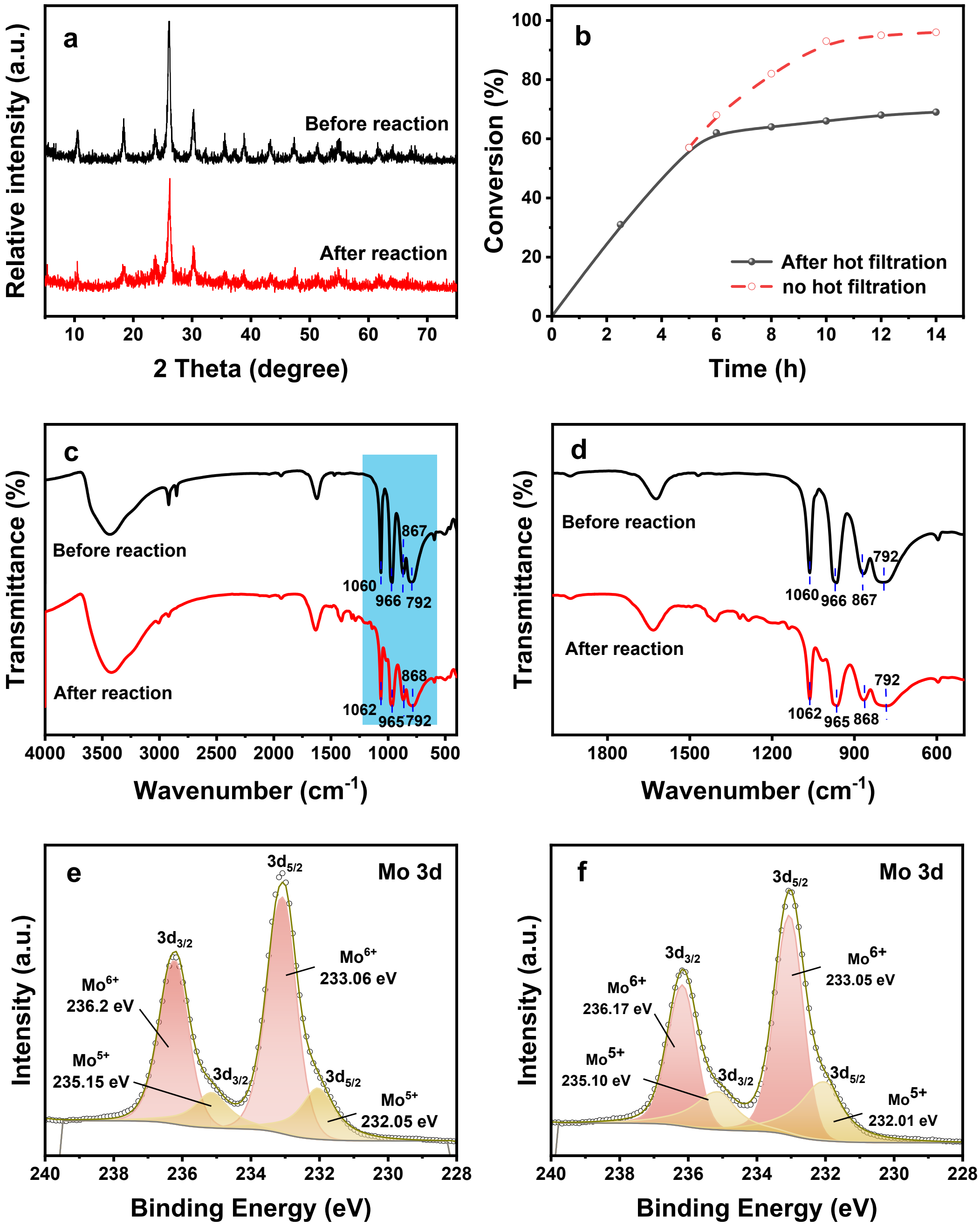

Fig. S4. Catalytic recyclability of 0.5 % Fe/Cs-PMA (a) XRD patterns of the fresh and spent catalyst. (b) After the catalyst was removed from the reaction system after reacting for 5 h, the filtrate continued to remain under the same condition. Reaction condition: 0.5 mmol PP-ol, 50 mg 0.5 % Fe/Cs-PMA, 4 mL DMSO, 140 °C, 1 MPa O_2. (c-d) FT-IR spectra of the catalyst and the enlarged light blue area. (e-f) XPS spectra of Mo 3d over

2.0% Fe/Cs-PMA before and after reaction.

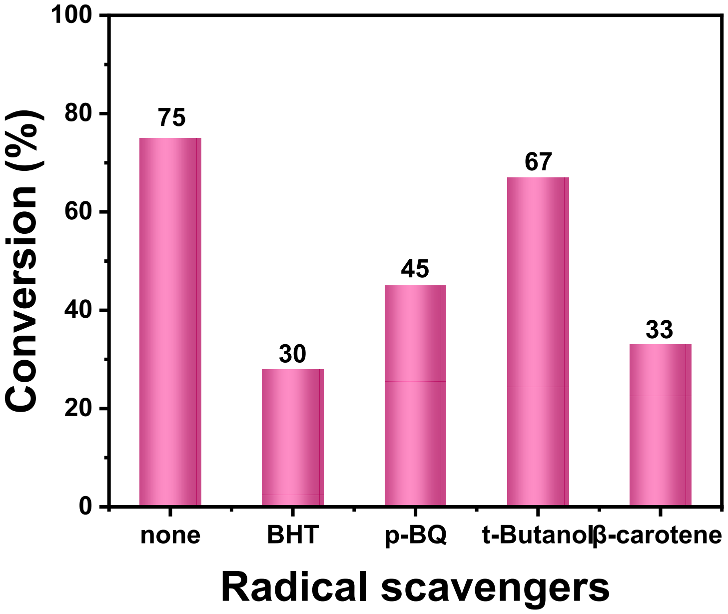

Fig. S5. Control experiments with different radical scavengers. Reaction condition: 0.5 mmol substrate, 50 mg 0.5 % Fe/Cs-PMA, 4 mL DMSO, 1.0 MPa O_2, 6 h, 1% (m/m) radical scavenger.

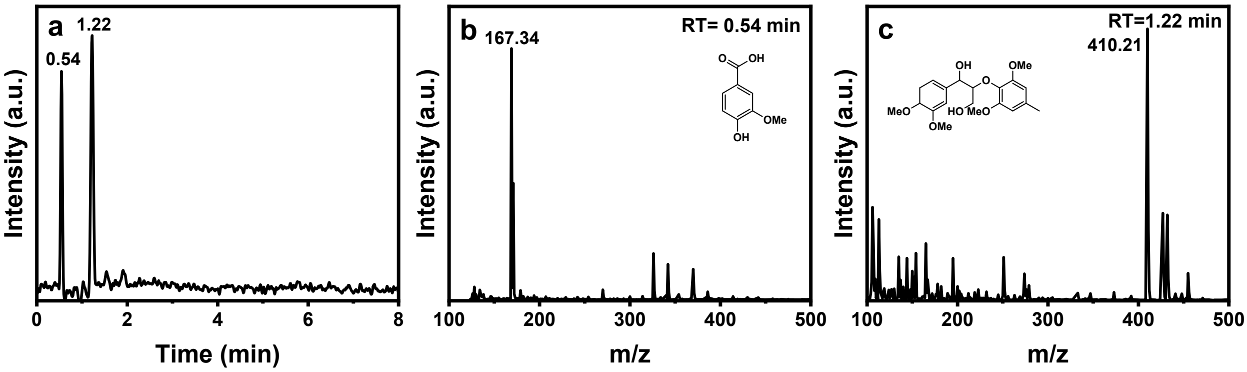

Fig. S6. HPLC-MS spectra of birch lignin degradation over 0.5 % Fe/Cs-PMA catalyst. (a) HPLC chromatogram (FTMS + p ESI Full ms 100-1000) of HPLC-MS, (b) Mass spectrum of HPLC-MS at tR=0.54 min, (c) Mass spectrum of HPLC-MS at tR=1.22 min.

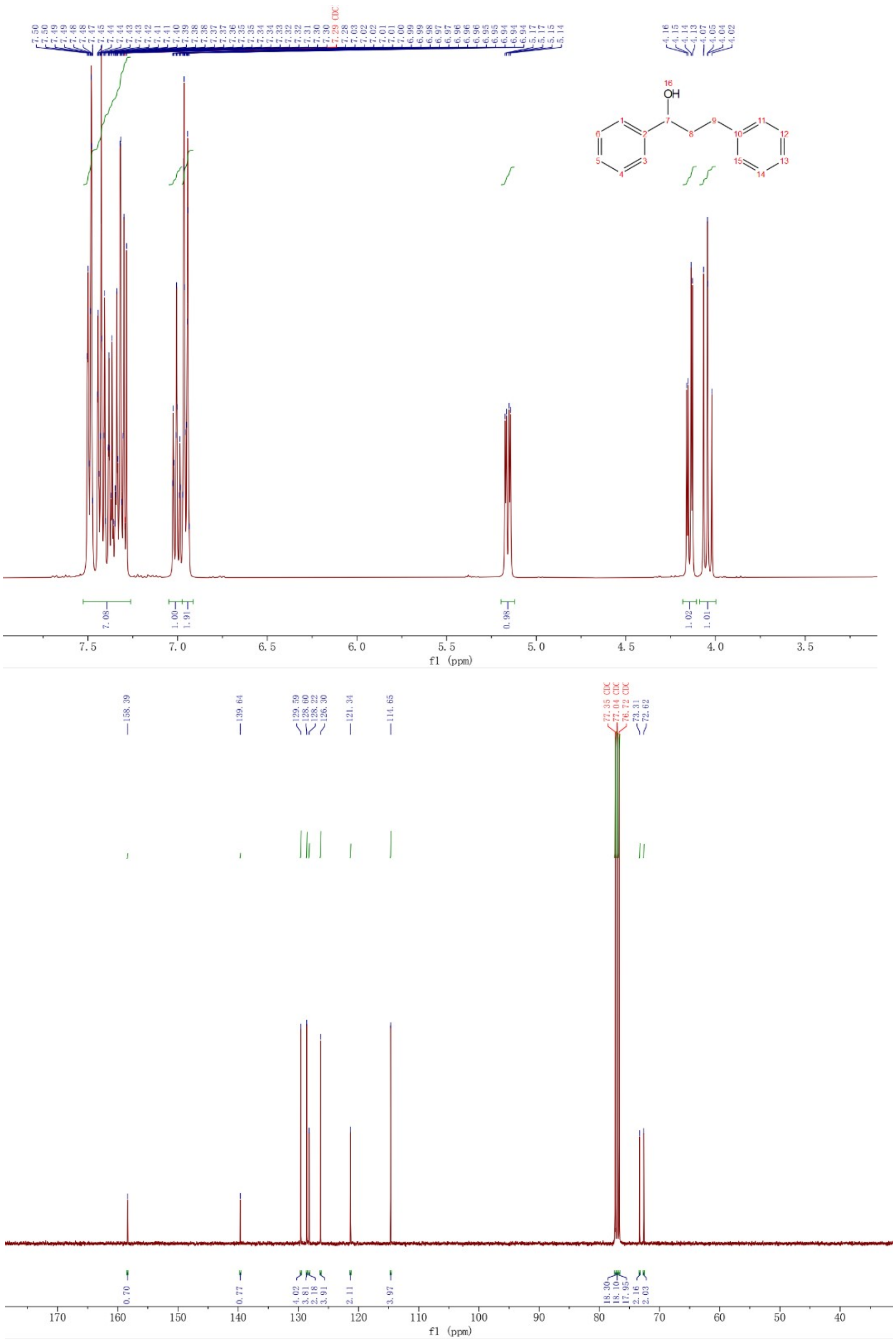

Fig. S7. Top) ^{1}H-NMR and bottom) ^{13}C-NMR spectrum of 2-phenoxy-1- phenylethanol.

^{1}H NMR (400 MHz, $CDCl_3$) δ 7.44 (d, 2H), 7.38 (t, 2H), 7.33 (d, 1H), 7.28 (dd, 2H), 6.97 (t, 1H), 6.92 (d, 2H), 5.10 (dd, 1H), 4.08 (dd, 1H), 4.00 (t, 1H), 2.81 (s, 1H). ^{13}C NMR

(101 MHz, $CDCl_3$) δ 158.34, 139.64, 129.54, 128.55, 128.16, 126.28, 121.36, 114.61, 73.25, 72.55. Spectral data are consistent with those reported in the literature.

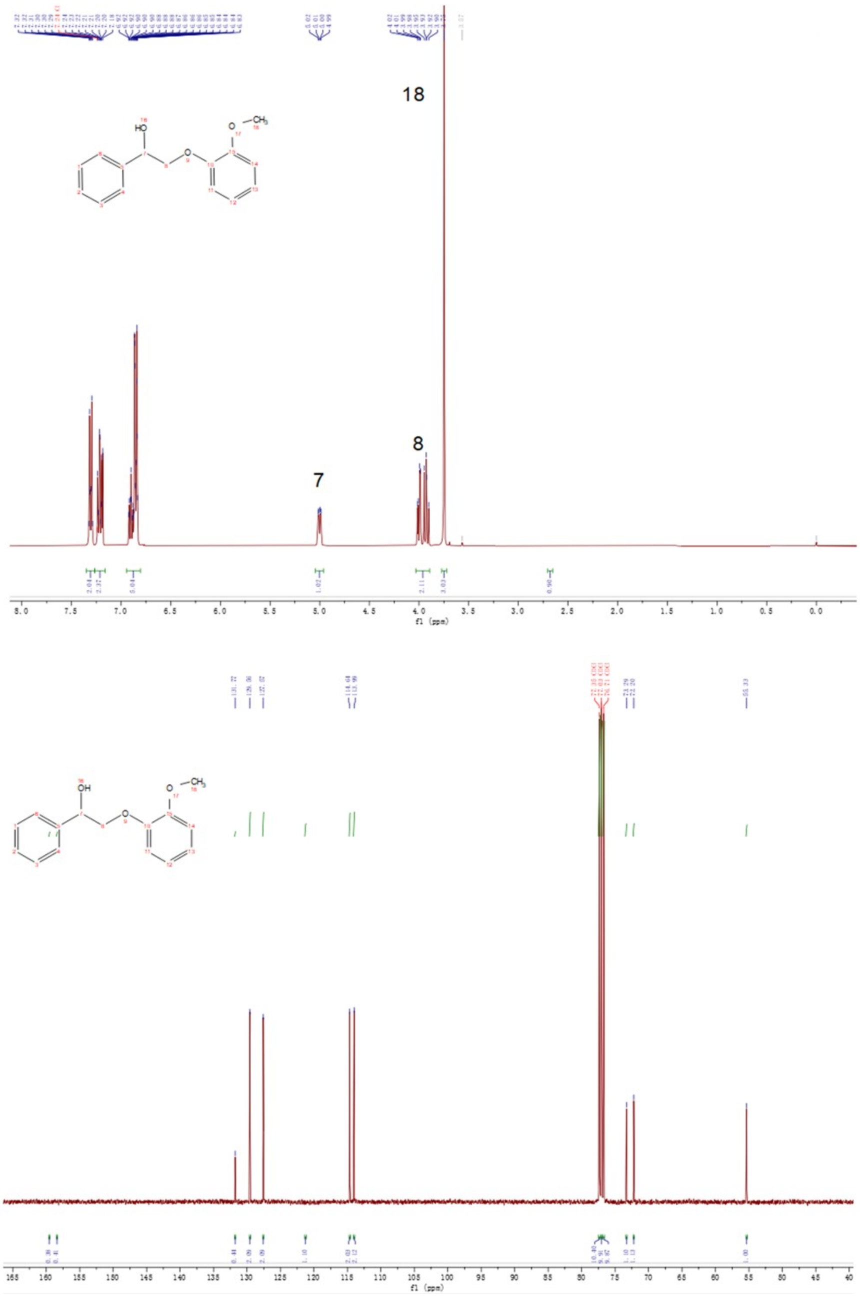

Fig. S8. Top) ^{1}H-NMR and bottom) ^{13}C-NMR spectrum of 2-(2-methoxyphenyl)-1-phenylethanol.

^{1}H-NMR (400 MHz, $CDCl_3$) δ 7.43 (d, 2H), 7.37 (t, 3H), 7.31 (t, 1H), 6.97 (t, 1H), 6.92 (t, 3H), 5.10 (dd, 1H), 4.16 (dd, 1H), 3.98 (t, 1H), 3.87 (s, 3H). ^{13}C NMR (101 MHz,

$CDCl_3$) δ 148.93, 146.91, 138.53, 127.44, 126.96, 125.26, 121.39, 120.06, 114.64, 110.92, 75.10, 71.27, 54.79. Spectral data are consistent with those reported in the literature.

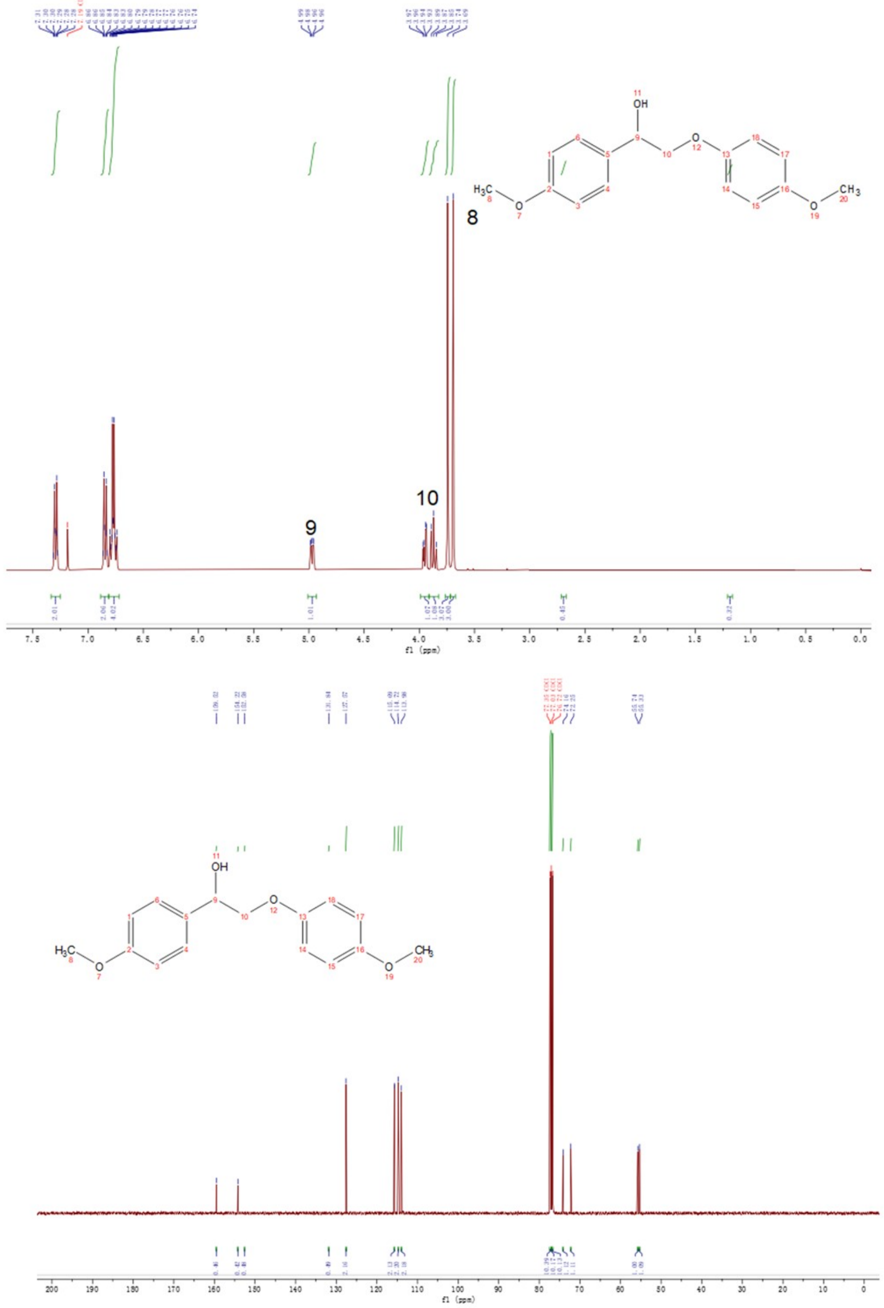

Fig. S9. Top) ^{1}H-NMR and bottom) ^{13}C-NMR spectrum of 1-(4-methoxyphenyl)-2- (4-methoxyphenyl)-phenoxyethanol.

^{1}H NMR (400 MHz, $CDCl_3$) δ 7.36 (d, 2H), 6.92 (d, 2H), 6.85 (d, 2H), 6.83 (d,2H), 5.03

(dd, 1H), 4.00 (dd, 1H), 3.94 (t, 1H), 3.81 (s, 3H), 3.76 (s, 3H). ^{13}C NMR (101 MHz, $CDCl_3$) δ 159.49, 154.17, 152.56, 131.85, 127.64, 127.53, 115.47, 114.51, 113.80, 74.12, 72.35, 55.90, 55.52. Spectral data are consistent with those reported in the literature.

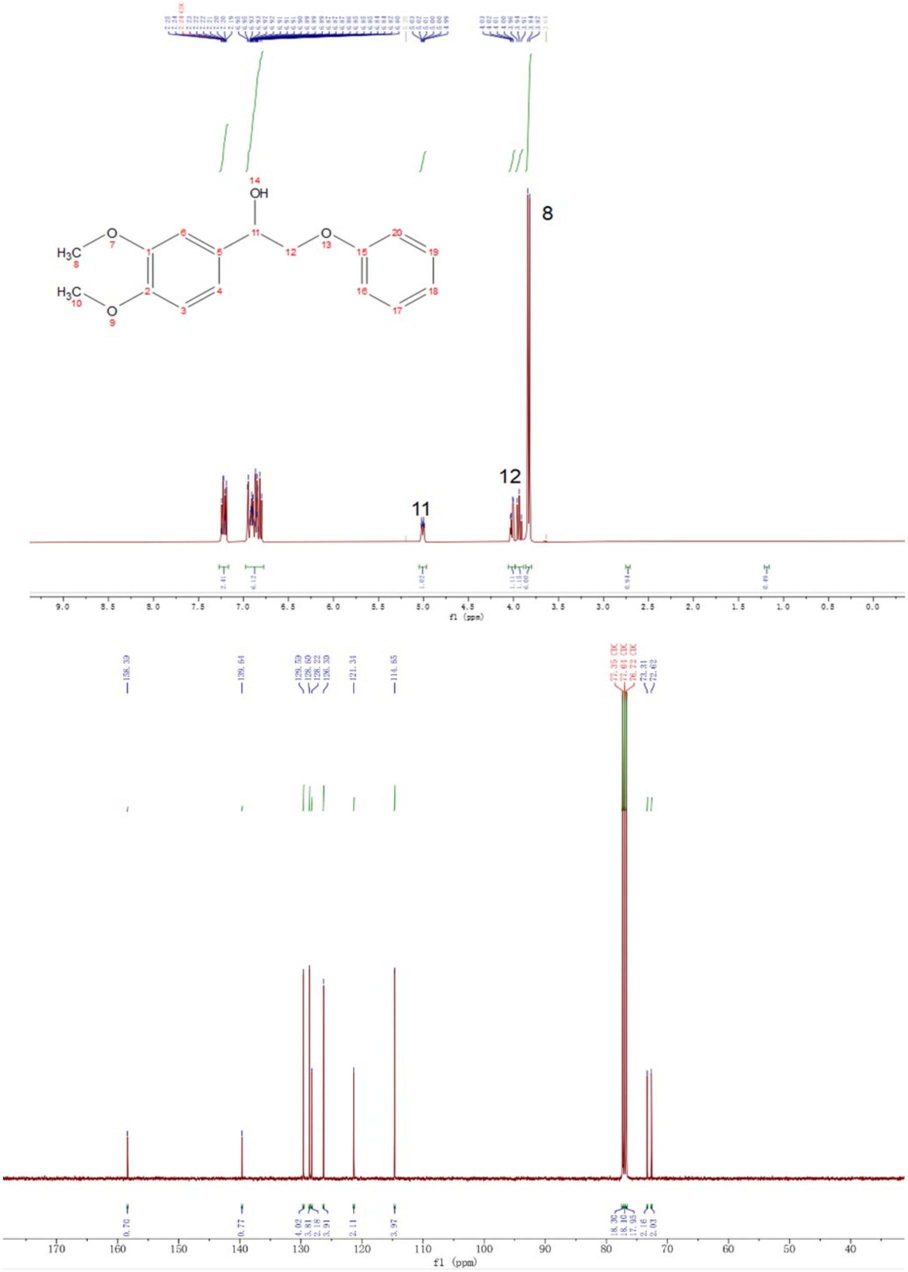

Fig. S10. Top) ^{1}H-NMR and bottom) ^{13}C-NMR spectrum of 1-(3,4- dimethoxyphenyl)-2-phenoxyethanol.

^{1}H NMR (400 MHz, $CDCl_3$) δ7.29 (m, 2H), 7.03 (m, 1H), 6.97 (m, 2H), 6.93 (m, 2H), 6.88 (m, 1H), 5.06 (dd, 1H), 4.07 (dd, 1H), 4.00 (m, 1H), 3.90 (s, 3H), 3.88 (s, 3H). ^{13}C NMR

(101 MHz, CDCl$_3$) δ 157.35, 148.09, 147.84, 131.40, 128.54, 120.27, 117.59, 113.60, 110.03, 108.31, 72.31, 71.35, 54.92, 54.87. Spectral data are consistent with those reported in the literature.

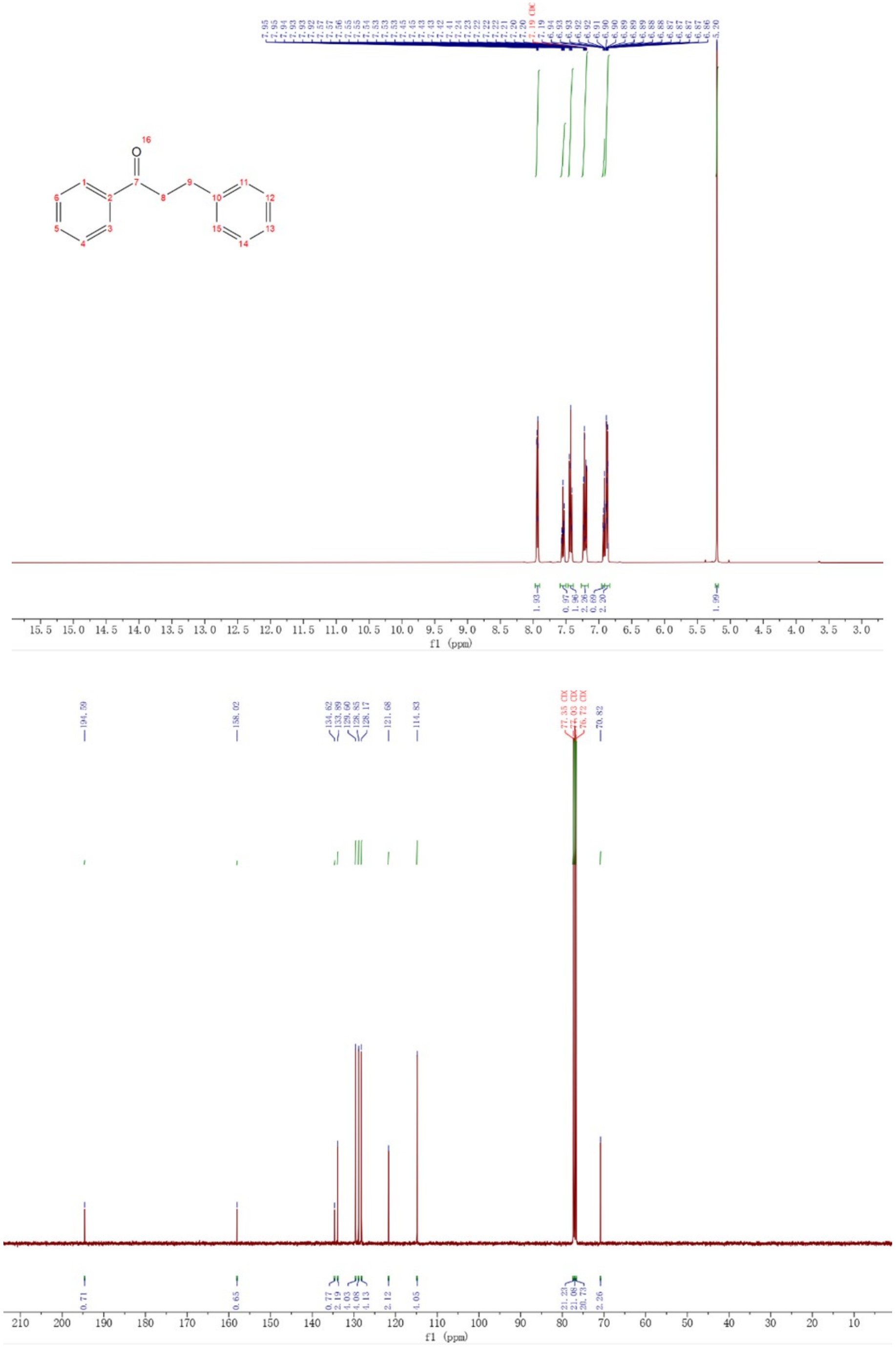

Fig. S11. Top) ^{1}H-NMR and bottom) ^{13}C-NMR spectrum of 2-phenoxy-1-phenylethanone. ^{1}H NMR (400 MHz, CDCl$_3$) δ 8.01 (s, 1H), 7.99 (s, 1H), 7.61 (t, 1H), 7.49 (t, 2H), 7.28 (t, 2H), 6.98 (t, 2H), 6.95 (d, 1H), 5.27 (s, 2H). ^{13}C NMR (101 MHz, $CDCl_3$) δ 194.54, 157.98, 134.56, 133.88, 129.58, 128.83, 128.13, 121.65, 114.79, 70.75. Spectral data are consistent with those reported in the literature.

References

1 W. Deng, H. Zhang, X. Wu, R. Li, Q. Zhang and Y. Wang, *Green Chemistry*., 2025, **17**, 5009-5018.

2 P. Lei, J. Zhang, W. Shen, M. Zhong and S. Guo, *Green Chemistry*., 2024, **26**, 6616-6624.

3 W. Song, Q. Dong, L. Hong, Z. Tian, L. Tang, W. Hao and H. Zhang, *RSC Adv*., 2019, **9**, 31070.

4 Q Wang, Y Liu, Y Jiang, Y Chen, Y Li, Y Zhang, X Wang, *Journal of colloid and interface science*., 2024, **682**, 263-274.

5 A Zhang, Y Ma, S Mao, R Zhang, Y Yuan, J Wang, Y Zhu, Z Wu, Y Sun, *ACS Sustainable Chemistry & Engineering*., 2025, **13**, 4623-4629.

6 Y. Wang, B, Ding, J. He, Z Ding and Z. Hou, *Energy & Fuels*., 2023, **37**, 5429-5440.